Analysis Framework of RSA Algorithms in Elastic Optical Rings

Haitao Wu, Fen Zhou, *Senior Member, IEEE*, Zuqing Zhu, *Senior Member, IEEE*, Yaojun Chen

***Abstract*—With flexibility in optical layer, Elastic Optical Network (EON) has been considered as a competitive candidate to architect next-generation backbone networks. Routing and Spectrum Assignment (RSA) is a key problem for the service provisioning in EONs. The RSA problem is $\mathcal{NP}$-hard even in elastic optical rings. Numerous heuristics have been proposed, and they can generally be categorized into two types: Route-First (RF) and Spectrum-First (SF). Although most previous work demonstrated by numerical simulations that the SF algorithms always outperform the RF ones, there is a lack of theoretical analysis on the reasons causing the performance difference between the two types of RSA algorithms. In this work, we aim at proposing a unified theoretical framework for the performance analysis of RSA algorithms by leveraging conflict graphs, which offers a new perception on the optimality of RSA algorithms. To validate the proposed framework, we apply it in elastic optical rings (with cycle topology), and theoretically analyze the number of edges of the conflict graphs for RF and SF algorithms. Different from the literature, we obtain an interesting observation that neither the RF nor the SF can surpass the other in elastic optical rings under different traffic distributions, and their performances have a strong correlation to the edge count of their conflict graph. This observation provides a new perspective, *i.e.* conflict graph, to explore the property of RSA algorithms.**

***Index Terms*—Elastic Optical Networks (EONs), Routing and Spectrum Assignment (RSA), Conflict Graphs, Rings**

I. Introduction

NOWADAYS, with diverse bandwidth-hungry applications deployed in the backbone networks, the demands of traffic bandwidths are growing exponentially. However, current Wavelength-Division-Multiplexing (WDM) networks, due to the coarse granularity of channels (typically at 50 or 100 GHz) [1], have been considered rigid with limited elasticity and flexibility in optical layer. Whereas the spectrum resources in optical layer are finite, the desire of developing highly-efficient and flexible optical networking technologies has stimulated intensive research interests [2, 3]. Elastic Optical Networks (EONs), due to the nature of flexible-grid, can achieve efficient and agile utilization of spectrum resources and have been considered as promising replacements to architect next-generation backbone networks [1, 4, 5]. In an EON, the spectrum resources on each fiber link are divided into narrow-band (*i.e.*, 12.5 GHz or less) Frequency Slices (FSs), with which the EON can allocate just-enough bandwidths to satisfy each connection request adaptively [6, 7]. Therefore, the spectrum utilization can be effectively improved in EONs in contrast to WDM optical networks.

The critical problem to realize the service provisioning in EONs is Routing and Spectrum Assignment (RSA) [8]–[11], *i.e.*, how to find a routing path and assign a block of available FSs on it to set up a lightpath for each connection request. Different from Routing and Wavelength Assignment (RWA) in WDM networks, which uses fixed channel sizes, the RSA has to deal with various channel sizes due to the flexible grids [10]. Hence, it is more challenging to solve the RSA problem, which has been proven to be $\mathcal{NP}$-hard even in elastic optical rings [8, 12]. To this end, numerous heuristic algorithms have been proposed to solve it time-efficiently. Note that, no matter how an RSA heuristic operates, it can be categorized into one of the two types, *i.e.*, Route-First (RF) algorithms and Spectrum-First (SF) ones. Specifically, RF algorithms solve the routing subproblem first and then allocate spectrum resources, while SF ones tackle RSA problem in an opposite way. The details regarding the two types of RSA heuristics will be discussed later in Section IV. For a comprehensive survey on heuristic RSA algorithms, one is suggested to refer to [13].

Apparently, the performance of service provisioning in EONs would be significantly affected by the used RSA algorithm. Most of current studies in literature [12, 14] demonstrated by numerical simulations that the performances of SF algorithms are always better than RF ones. But numerical results can be easily biased by many factors such as traffic distributions and EON topologies. Therefore, solid theoretical works to analyze the two types of RSA algorithms in a united framework are needed.

In this work, we focus on the performance evaluation of RSA algorithms rather than proposing new ones. We aim at developing a unified theoretical framework for the performance analysis of RSA algorithms by leveraging conflict graph. More specifically, the conflict graph of an RSA algorithm is an auxiliary graph that describes the intersections among the routing paths computed by it. The main contributions of this work are summarized as follows:

- By leveraging conflict graph, we propose a united framework in which all RSA algorithms (RF and SF) can be regarded as first solving routing subproblem and then allocating spectrum resources.
- We show that the performance of an RSA algorithm is restricted by the number of edges of its conflict graph.

H. Wu is with the CERI-LIA at the University of Avignon, France. He is also with the Department of Mathematics, Nanjing University, Nanjing 210093, China. (email: haitao.wu@alumni.univ-avignon.fr).

F. Zhou is with the LISITE lab of Institut Supérieur d'Électronique de Paris. He is also with the CERI-LIA lab at the University of Avignon, France. (email: fen.zhou@{isep, univ-avignon}.fr).

Z. Zhu is with the School of Information Science and Technology, University of Science and Technology of China, Hefei, Anhui 230027, China. (e-mail: zqzhu@ieee.org).

Y. Chen is with Department of Mathematics, Nanjing University, Nanjing 210093, China. (email: yaojunc@nju.edu.cn).

To validate this framework, we apply it in elastic optical rings, and theoretically analyze the number of edges of the conflict graphs of RF and SF algorithms under concentration and uniform traffic distributions. To the best of our knowledge, it is the first time that this framework and this kind of theoretical analysis are proposed.

- Different from the results claimed in the literature, we obtain an observation that neither the RF nor the SF can dominate the other in elastic optical rings. In fact, the RF consumes less spectrum for uniform traffic distribution, while it is inverse for the concentration distribution.

The rest of this paper is organized as follows. Section II briefly introduces related work and our motivation. We formally formulate RSA problem and give the definition of conflict graph in Section III. Two representative RSA algorithms selected respectively from the RF and the SF are discussed in Section IV. In Section V, we propose a unified theoretical analysis framework for RSA algorithms, and apply this framework in Section VI to theoretically analyze the properties of their conflict graphs in elastic optical rings under two traffic distributions. We conduct simulations in Section VII to further verify our analysis. Finally, Section VIII summarizes this paper.

II. Related Work and Motivation

With the help of efficiency, flexibility, and scalability, EONs have been considered as promising candidates to support future Internet cost-efficiently. The RSA [8, 9] is a central problem for service provisioning in EONs. It can be naturally separated into two subproblems: lightpath routing and spectrum assignment. Many RSA algorithms have been proposed. Based on the priority of solving the two subproblems, RSA algorithms can be generally classified into two types: RF and SF. In [15], the authors proposed an RSA heuristic that uses the shortest path with maximum spectrum reuse (**SPSR**) to solve the routing subproblem first. Meanwhile, people also proposed to use a layered approach to design an integrated layered approach (**ILA**) RSA algorithm [14], which tried to solve the spectrum assignment subproblem first. Besides the basic RSA problem, many variants of the RSA have been proposed in the literature. In [16]–[18], the authors investigated the RSA problem for multicast communications. In [19], the authors took into account the physical-layer security for solving the RSA problem. A comprehensive survey of RSA algorithms can be found in [13]. In addition, spectrum fragmentation is a major obstacle to the efficient utilization of spectrum resources in EONs [20]. To tackle this problem, many theoretical works have been proposed [21]–[23]. In [23], the authors put forward a novel defragmentation scheme that allows both the primary and the backup lightpaths, to be reallocated during the defragmentation process so as to improve the spectrum utilization. A comprehensive survey on the spectrum fragmentation can be founded in [24]. Moreover, virtual network embedding is also studied in EONs to enhance its performance [25].

For the basic RSA problem in EONs, most studies in literature [12, 14] claimed that SF algorithms are always better than RF ones in their numerical simulations. But each RSA algorithm would have pros and cons, and a united framework would be desirable to analyze them clearly. To the best of our knowledge, there has been no previous work on this topic. On the other hand, RSA problem is a $\mathcal{NPC}$-problem even in elastic optical rings [12], and the optical rings are widely deployed for metro networks and some long haul networks. Thus, a united theoretical analysis in elastic optical rings is also of theoretical and practical meanings.

In this work, from the point of view of conflict graph, we unify the two types of RSA algorithms in a same framework, and focus our work in elastic optical rings to theoretically analyze the performance of two representative RSA algorithms.

III. RSA Problem and Conflict Graph

A. Formulation of RSA

In this paper, we use a bidirected graph $G(V, E)$ to represent the topology of an EON, where V and E denote the sets of nodes and edges respectively. Each edge in E contains two directed fiber links (arcs) with one for each direction. A set of FSs lies on each directed fiber link as shown in Fig. 1.

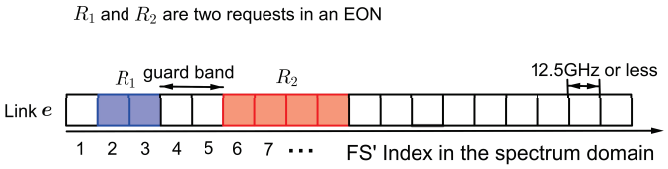

Fig. 1. FSs and guard-bands in a fiber link of an EON.

TABLE I
Notations

$G(V, E)$	The underlying EON, where V is the set of nodes, and E is the set of directed link fibers.
$\mathbb{N}^+$	The set of positive natural numbers representing the FS index set in the spectrum domain lying in each directed fiber link $e \in E$.
$\mathcal{R}$	The set of connection requests in $G(V, E)$.
n	$= \lvert\mathcal{R}\rvert$, the number of connection requests.
$R_i(s_i, d_i)$	$R_i \in \mathcal{R}$ representing the i-th connection request,where $s_i, d_i \in V$ are the source and destination nodes respectively.
R_i^w	The integer weight indicating the number of contiguous FSs (bandwidth requirement) required by R_i.
$\mathcal{P}_i$	The set of all the possible directed lightpaths from s_i to d_i in $G(V, E)$.
P_i	$P_i \in \mathcal{P}_i$ is the directed lightpath selected to R_i.
W_i	The set of contiguous FSs assigned to R_i.
R_i^b	$R_i^b \in \mathbb{N}^+$ is the start-index of W_i.
R_i^a	$R_i^a \in \mathbb{N}^+$ is the end-index of W_i.
GB	$GB \in \mathbb{N}^+$ is the number of FSs of the guard-band.
MUFI	$= \max_{s \in (\cup W_i)}(s)$, the maximum used FS index.
$\hat{G}(\hat{V}, \hat{E})$	The conflict graph which is a weighted undirected graph, where $\hat{V}$ is the vertex set corresponding to $\mathcal{R}$, and $\hat{E}$ is the edge set.
$\hat{v}_i$	$\hat{v}_i \in \hat{V}$ corresponds to R_i.
$\hat{v}_i^w$	$= R_i^w$, the vertex weight of $\hat{v}_i$.
$W_{\hat{v}_i}$	The set of contiguous FSs assigned to $\hat{v}_i$.
$\hat{v}_i^b$	$\hat{v}_i^b \in \mathbb{N}^+$ is the start-index of $W_{\hat{v}_i}$.
$\hat{v}_i^a$	$\hat{v}_i^a \in \mathbb{N}^+$ is the end-index of $W_{\hat{v}_i}$.

The bandwidth required by a request is measured by a number of FSs. When a connection request arrives, the EON

needs to set up a directed lightpath and assigns enough FSs on it to forward data. For ease of expression, we formally give some notations in Table I.

Given a set $\mathcal{R} = \{R_i\}_{i=1}^{n}$ of requests, RSA problem is to select a lightpath P_i from $\mathcal{P}_i$ and assign an appropriate FS set W_i for each R_i while satisfying the following constraints:

- **Bandwidth Requirement Constraint**. The number of FSs assigned to each request should satisfy the bandwidth requirement, *i.e.*, the cardinality of W_i assigned to R_i must be equal to its weight:

$$|W_i| = R_i^w, \quad \forall R_i \in \mathcal{R}. \tag{1}$$

- **Spectrum Contiguity Constraint**. The FSs assigned to request R_i must be contiguous in $\mathbb{N}^+$. Then, W_i can be expressed as $\{R_i^b, R_i^b + 1, ..., R_i^a - 1, R_i^a\}$. This is a physical layer constraint for all-optical communications.
- **Spectrum Continuity Constraint**. The set of contiguous FSs W_i assigned to R_i in each link $e \in P_i$ must be the same.
- **Guard Band Constraint**. To mitigate mutual interference, when P_i and P_j share common directed fiber links, the distance between W_i and W_j in the spectrum domain should not be less than GB (as shown in Fig. 1):

$$distance(W_i, W_j) \geq GB, \quad \forall P_i \cap P_j \neq \emptyset, \tag{2}$$

where,

$$distance(W_i, W_j) = \min_{s \in W_i, t \in W_j} (|s - t| - 1).$$

Here, it should be noted that the GB can be any non-negative integers, whose value can be determined according to the interference levels [10].

For the objective of the RSA problem, two variants have been studied in the literature: max-RSA and min-RSA [26]. For the former problem, the focus is on the provisioning over an EON under limited spectrum resource, and the objective is to maximize the number of connection requests that can be served. The latter one has a planning concern and its objective is to minimize the required spectrum usage to serve all the connection requests. In this paper, we focus on the static network planning problem, and it is very common to assume that the spectrum resources are sufficient in the phase of network planning [27]. Thus, the objective is to minimize the maximum used FS index (MUFI), which can be expressed by Eq. (3). **Objective Function:**

$$\min \left[\max_{s \in (\cup W_i)} (s) \right] \qquad (\textbf{RSA}). \tag{3}$$

B. Conflict Graph

Conflict graph is a useful tool to analyze RSA algorithms in the study of optical networks, which is an auxiliary graph to depict the intersections among the set of lightpaths $\{P_i\}_{i=1}^{n}$ selected for $\{R_i\}_{i=1}^{n}$. We formally give its definition in the following.

Definition 1: The conflict graph [28] $\hat{G}(\hat{V}, \hat{E})$ of an RSA algorithm is **a weighted undirected graph** whose vertex set $\hat{V}$ represents the set of requests, *i.e.*, $\mathcal{R}$. Any two vertices $\hat{v}_i, \hat{v}_j \in \hat{V}$ (represent R_i and R_j respectively) are connected by an edge $\hat{e} \in \hat{E}$, iff P_i **intersects with** P_j, *i.e.*, $P_i \cap P_j \neq \emptyset$ **(at least one directed fiber link shared by** P_i **and** P_j**)**. We denote the weight of vertex $\hat{v}_i$ by $\hat{v}_i^w$, and $\hat{v}_i^w = R_i^w$. Besides, $\hat{v}_i^b$, $\hat{v}_i^a$ and $W_{\hat{v}_i}$ have the same meanings as R_i^b, R_i^a and W_i respectively. If $\hat{v}_i$ and $\hat{v}_j$ are adjacent in $\hat{G}$, the distance between $W_{\hat{v}_i}$ and $W_{\hat{v}_j}$ should be no less than GB.

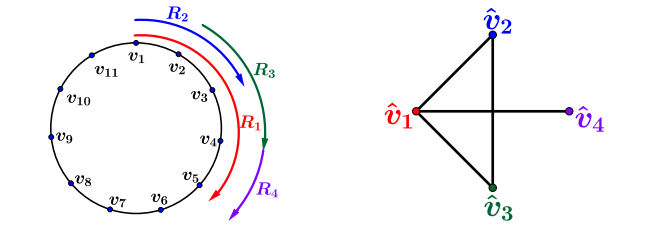

(a) Selected paths. (b) The conflict graph.

Fig. 2. Routing Phase of the RF algorithm.

Figure 2(b) showcases a 4-node conflict graph for the 4 connection requests in Fig. 2(a), where $\hat{v}_i$ corresponds to $R_i, \forall 1 \leq i \leq 4$. According to the definition, obviously, any proper spectrum assignment for the conflict graph corresponds to a proper spectrum assignment for the requests, vice versa. Thus, the conflict graph embodies all the four constraints of RSA mentioned above, and is very important to analyze the RSA problem. Given a set of connection requests $\mathcal{R}$, no matter how they are routed, we can use the conflict graph to characterize the intersections among them.

IV. The Route-First and Spectrum-First Algorithms

To approach the optimal MUFI, most RSA algorithms improve their performances from two aspects *i.e.*, **routing phase** and **spectrum assignment phase**. Among them, the representative RSA algorithms (one for each type) mentioned above, *i.e.*, SPSR [15] and ILA [14], are used as our benchmark algorithms.

A. RF Algorithm

In SPSR algorithm [15], each $R_i \in \mathcal{R}$ is routed by the shortest path. A conflict graph $\hat{G}(\hat{V}, \hat{E})$ is constructed based on these routing paths, and then a maximum reuse spectrum allocation (MRSA) algorithm is used. The main idea of MRSA is to: (1) sort $\hat{v} \in \hat{V}$ in the descending order of $\hat{v}^w$; (2) select the vertex $\hat{v}_i$ with the biggest weight but not yet assigned with FSs, and allocate the first available $W_{\hat{v}_i}$ to $\hat{v}_i$ (*i.e.*, the start-index $\hat{v}_i^b$ is as small as possible); (3) select those vertices, which are not yet assigned with FSs and compose an independent set[1] with $\hat{v}_i$, and allocate the first available FS sets to them; (4) repeat the same process until all vertices in $\hat{V}$ are assigned with FS sets.

[1]An independent set is a set of vertices, no two of which are adjacent in the conflict graph $\hat{G}(\hat{V}, \hat{E})$.

The SPRS algorithm is a typical RSA algorithm, which gives priority to the routing phase for saving fiber link resources. Thus, we name it as Route-First (RF) algorithm in our paper. Figures 2 and 3 demonstrate the whole process of the RF algorithm. The required bandwidths of $R_1(v_1, v_5)$, $R_2(v_1, v_3)$, $R_3(v_2, v_4)$ and $R_4(v_4, v_5)$ are 3 FSs, 3 FSs, 2 FSs and 1 FS respectively, and $GB = 1$. The routing phase and the conflict graph are shown in Figs. 2(a) and 2(b) respectively.

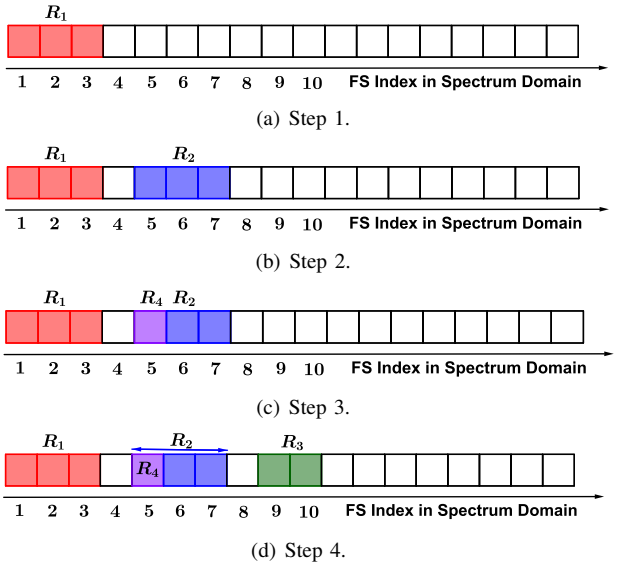

(a) Step 1.

(b) Step 2.

(c) Step 3.

(d) Step 4.

Fig. 3. Spectrum assignment phase of the RF algorithm.

The spectrum assignment phase is shown in Fig. 3. According to the vertex weights, the vertex order is $(\hat{v}_1, \hat{v}_2, \hat{v}_3, \hat{v}_4)$. First, R_1 is assigned the first available $W_1 = \{1, 2, 3\}$. As $\hat{v}_1$ is adjacent to the remaining vertices, no vertex composes an independent set with $\hat{v}_1$. Then, the process continues, and $\hat{v}_2$ is the vertex with the biggest weight. R_2 is assigned with the first available $W_2 = \{5, 6, 7\}$. Since $\hat{v}_4$ and $\hat{v}_2$ compose an independent set, R_4 is assigned with the first available $W_4 = \{5\}$. Finally, R_3 is assigned with $W_3 = \{9, 10\}$ and the MUFI is 10. The time complexity of routing phase and spectrum assignment phase of the RF are $\mathcal{O}(n * |V|^2)$ and $\mathcal{O}(n \log n + n^2)$ respectively. Therefore, the overall time complexity of the RF is $\mathcal{O}(n * |V|^2 + n^2)$.

B. Spectrum-First Algorithm

Given an EON $G(V, E)$, ILA algorithm [14] assumes that there are F FS indices lying in each fiber link $e \in E$. Thus, each directed fiber link e can be viewed as parallel directed edges consisting of $\{e^1, e^2, ..., e^F\}$, where e^i represents the i-th FS index in link e and can be used by only one connection request. Naturally, the EON with F FSs on each fiber link can be regarded as a layered graph comprising of F identical layers $\{G^1(V^1, E^1), G^2(V^2, E^2), ..., G^F(V^F, E^F)\}$, where the initial topology of each layer is $G^i(V^i, E^i) = G(V, E)$.

In ILA algorithm, the requests are first sorted in the descent order of bandwidths, and then each request $R_i(s_i, d_i)$ is sequentially served in the following manner: (1) find the first R_i^w FS-contiguous layers in the F-layered network such that there is at least one common path from s_i to d_i in all these R_i^w layers; (2) route the request by using the shortest common directed path (may not be the shortest path in the original network), and assign the corresponding R_i^w FSs; (3) delete the used edges from these R_i^w layers and repeat the same procedure until all requests are accommodated. ILA algorithm is a typical RSA algorithm, which favors the minimization of FS index when accommodating a request. Thus, we call ILA Spectrum-First (SF) algorithm.

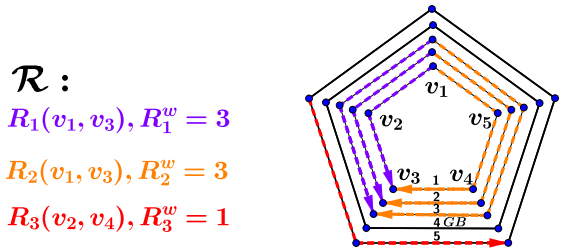

(a) The request set.

(b) Final Accommodations.

Fig. 4. An illustration of the Spectrum-First algorithm.

Figure 4 illustrates the process of the SF algorithm. We consider an elastic optical ring with 5 nodes in Fig. 4(b), where each edge contains two directed fiber links, while only the used ones have been drawn for ease of understanding. The three requests in Fig. 4(a) should be routed. Here, R_1 and R_2 are treated as different requests, and $GB = 1$. At the beginning, the EON is viewed as a layered graph and each layer represents one FS. There are in total 5 layers as shown in Fig. 4(b). First, R_1 is accommodated by the first three layers (purple arrows from inner to outer), and the corresponding arcs are deleted from these layers. As the SF algorithm aims at minimizing the number of FS used, it then uses a longer path rather than the shortest one to satisfy the request R_2. Similar processes are repeated for R_3. Figure 4(b) gives the final accommodations, where the MUFI is 5. The time complexity of the SF is $\mathcal{O}\big(n^2 * (|E| + |V|) + n * |V|^2\big)$ [14], which is bigger than the RF's.

V. Unified Theoretical Analysis Framework of RSA Algorithms based on Conflict Graph

Conflict graph is a useful tool to analyze RSA algorithms. No matter what RSA algorithms is used, we can use the conflict graph to characterize its routing phase, which has a decisive impact on its final performance. This point can be exemplified by the two benchmark algorithms.

For the RF algorithm, the conflict graph is clear, which is constructed in line with the intersections of the lightpaths at the routing phase. While the conflict graph for the SF algorithm may be not clear, because routing and spectrum assignment phases are integrated together. However, after all connection requests are accommodated, we can also construct the conflict graph according to the intersections among the lightpaths. For example, the conflict graph of Fig. 4(b) is given in Fig. 5. Due to link directionality, v_4v_3 and v_3v_4 represent two distinct fiber links, and thus R_2 does not share any common (directed) fiber links with R_1 and R_3. Consequently, $\hat{v}_2$ is not connected to $\hat{v}_1$ and $\hat{v}_3$ in the conflict graph.

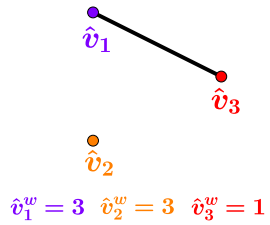

Fig. 5. The conflict graph of Fig. 4(b).

After sorting all connection requests in the descent order of bandwidths, the particularity of the SF algorithm is to sequentially route each request and assign enough FSs following the principle of making the start-index of the assigned FS set minimum. Actually, we can still reconstruct the solution of the SF algorithm by following a similar way as the RF: construct the conflict graph $\hat{G}$ based on all the computed routing paths by the SF algorithm and then use a special spectrum assignment scheme. Now, we have Theorem 1.

Theorem 1: Given a set of requests $\{R_i\}_{i=1}^n$, let O be the descent order of bandwidths of requests and $\hat{G}(\hat{V}, \hat{E})$ be the conflict graph of the SF algorithm. Following the order O, we sequentially assign FS set $W_{\hat{v}_i}$ to each $\hat{v}_i \in \hat{V}$ by the principle that makes the start-index $\hat{v}_i^b$ minimum. The MUFI produced for $\hat{G}$ in such way is equal to that of the SF algorithm.

Proof. We will prove a stronger statement by induction: The FS set $W_{\hat{v}_i}$ assigned to each vertex $\hat{v}_i \in \hat{V}$ is the same as the W_i assigned to R_i by the SF algorithm. Without loss of generality, we suppose that the descent order O is $(R_1, R_2, ..., R_n)$ (the corresponding vertex order in $\hat{G}$ is $(\hat{v}_1, \hat{v}_2, ..., \hat{v}_n)$). At $i = 1$, it is easy to see that $W_{\hat{v}_i} = W_i$. Assuming this inference is true when $i = k$, where $k < n$, we assert $W_{\hat{v}_{k+1}} = W_{k+1}$. To prove this assertion, we just need to prove that $\hat{v}_{k+1}^b = R_{k+1}^b$.

First we prove $R_{k+1}^b \geq \hat{v}_{k+1}^b$. From the construction of $\hat{G}$, it is trivial that $\forall r \leq k$, the lightpath P_r of R_r intersects with the lightpath P_{k+1} of R_{k+1} iff $\hat{v}_r$ is adjacent to $\hat{v}_{k+1}$ in $\hat{G}$. The FS set W_{k+1}, whose FS start-index is R_{k+1}^b, respects the guard-band constraint with request $R_r, \forall r \leq k$, whose lightpath $P_r \cap P_{k+1} \neq \emptyset$. Thus, if we assign W_{k+1} to $\hat{v}_{k+1}$, it will also satisfy the guard-band constraint with vertex $\hat{v}_r, \forall r \leq k$ which is adjacent to $\hat{v}_{k+1}$ in $\hat{G}$. Therefore, by the minimality of $\hat{v}_{k+1}^b$, we have $R_{k+1}^b \geq \hat{v}_{k+1}^b$.

With the fact mentioned above, we can also prove $R_{k+1}^b \leq \hat{v}_{k+1}^b$ by the minimality of R_{k+1}^b in the similar way. Therefore, $\hat{v}_{k+1}^b = R_{k+1}^b$ and the proof follows. ■

Here, we illustrate the proof of Theorem 1 by the assigning FS set to the conflict graph in Fig. 5. Obviously the descent order O of bandwidths is $(\hat{v}_1, \hat{v}_2, \hat{v}_3)$. Following the order O, we sequentially assign FS set $W_{\hat{v}_i}$ to each $\hat{v}_i \in \hat{V}$ by the principle that makes the start-index $\hat{v}_i^b$ minimum. The details are illustrated as follows. Comparing the FS sets in Figs. 4(b) and 6, they are indeed the same for each request.

Now, let us review the processes of the RF algorithm and the SF algorithm again:

- The RF algorithm:
  (1) Construct a conflict graph $\hat{G}$ based on shortest paths;
  (2) Use MRSA algorithm to optimize the MUFI in $\hat{G}$.
- The SF algorithm, by the equality proved in Theorem 1, can be also regarded as:
  (1) Construct a conflict graph $\hat{G}$ based on the routing paths computed by the SF;
  (2) Assign FS sets following the descent order of bandwidths to optimize the MUFI in $\hat{G}$.

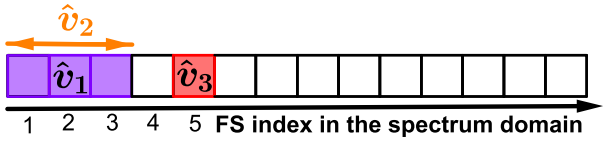

Fig. 6. Spectrum assignment of the conflict graph in Fig. 5.

In fact, all RSA algorithms can be discussed in the united framework from conflict graph:

- **(i)** Construct a conflict graph $\hat{G}$ by some way;
- **(ii)** Assign FS sets by different methods.

Thus, the conflict graphs has a decisive impact on the final MUFI produced by an RSA algorithm. From the definition, the edges of a conflict graph actually represent the incompatibilities among the routing paths of connection requests. The more edges a conflict graph has, the more incompatible these routing paths, the bigger the final MUFI. This point can be observed by comparing the two conflict graphs in Figs. 2(b) and 5 and their finally MUFIs in Figs. 3 and 6. Naturally, the final performance of an RSA algorithm is deeply restricted by the number of edges of its conflict graph.

VI. Framework Application in Elastic Optical Rings

In EONs of some regular topologies such as cycle (*i.e.*, optical rings[2]), the number of edges of its conflict graph can be theoretically derived. As the edge number of the conflict graph may reflect some inherently topological characteristics of the EONs, they are important for analyzing the final performances. Here, we apply the proposed framework in elastic optical rings, whose topology is a cycle, and theoretically derive the number of edges in the conflict graphs built by the RF and the SF. All the theoretical analyses are derived in **odd-cycle elastic optical rings**, in which **the number of nodes is odd**. These results can be extended to the **even-cycle** case (**the number of nodes in the ring is even**) by trivial modifications. Besides the EON topology, the traffic distribution is also another important factor influencing the final performance. In some literature like [15], a uniform traffic distribution was adopted, while [29, 30] assumed that traffics are only concentrated on a certain part of EON nodes. In this paper, we thus consider two types of traffic distributions for comparison: concentration and uniform distributions. First, we give the detail of the two request distributions.

- Concentration distribution $\mathcal{D}_c$:
  Given an odd-cycle bidirectional elastic optical ring $G(V, E)$ and $V = \{1, 2, ..., 2M + 1\}$, whose vertex

[2]Hereafter, we use the terms cycle and ring interchangeably.

labels are sorted in the clockwise order, the concentration distribution $\mathcal{D}_c$ means that: for each connection request $R(s,d)$, s and d ($s \neq d$) are uniformly generated from $\{1,2,...,M,M+1\}$, *i.e.*, the source and destination are always concentrated in this semi-cycle.

- Uniform distribution $\mathcal{D}_u$:
  In an EON $G(V,E)$, the uniform request distribution $\mathcal{D}_u$ is that: the s and d ($s \neq d$) of each connection request $R(s,d) \in \mathcal{R}$ are generated from V with uniform probability. In this case, the requests are generated over the entire cycle rather than just a semi-cycle.

Since each request is generated according to a traffic distribution ($\mathcal{D}_c$ or $\mathcal{D}_u$), the edge number $|\hat{E}|$ of conflict graph $\hat{G}(\hat{V},\hat{E})$ can be viewed as a random variable. We denote by $\mathbf{E}(|\hat{E}|)$ the expectation of the number of the edges of the conflict graph $\hat{G}(\hat{V},\hat{E})$. Since $|\hat{V}| = |\mathcal{R}| = n$, there are $\binom{n}{2}$ possible edges in $\hat{E}$. Thus, according to the linearity of expectation, we have $\mathbf{E}(|\hat{E}|) = \binom{n}{2} \times p$, where p is the probability of any two $\hat{v}_i$ and $\hat{v}_j$ adjacent in $\hat{G}$, *i.e.*, the probability of intersecting of the lightpaths of any two request R_i and R_j.

A. Conflict Graph of the RF algorithm

1) In the concentration distribution $\mathcal{D}_c$:

Theorem 2: Suppose that an EON $G(V,E)$ is an odd-cycle bidirectional ring with $|V| = 2M+1$ and all of the requests in $\mathcal{R}$ generated from the $\mathcal{D}_c$ and that $\hat{G}(\hat{V},\hat{E})$ is the conflict graph of RF algorithm, then the $\mathbf{E}(|\hat{E}|)$ is $\binom{n}{2}\frac{M^4-7M^2-6M}{3M^4+6M^3+3M^2} = \binom{n}{2}(\frac{1}{3}+o(1))$, where n is the number of requests ($o(1)$ is an infinitesimal of M).

Proof. From the above analysis that $\mathbf{E}(|\hat{E}|) = \binom{n}{2} \times p$, we just need to calculate the p of any two requests R_i and R_j. According to the analysis above, p is the probability that $P_i \cap P_j \neq \emptyset$, where P_i and P_j are the shortest paths for R_i and R_j respectively. Under the concentration distribution, the request pair (R_i,R_j) has a total of $M^2(M+1)^2$ cases.

We construct a (0-1)-matrix $\mathcal{M}^p_{\mathcal{D}_c}$ as shown in Table II. The top row in Table II represents that all source-destination pairs are routed on their shortest paths, and the leftmost column is of the same meaning. One entry $((s_i,d_i),(s_j,d_j))$ of this matrix equals 1 iff the shortest path of (s_i,d_i) intersects with that of (s_j,d_j). Thus, it is easy to see that $p = \frac{\sum \mathcal{M}^p_{\mathcal{D}_c}}{M^2(M+1)^2}$,

TABLE II
(0-1)-MATRIX $\mathcal{M}^p_{\mathcal{D}_c}$

R_i \ R_j	.	.	(s_j,d_j)	.	.
.	.	.	.	.	.
.	.	.	.	.	.
(s_i,d_i)	.	.	1	.	.
.	.	.	.	.	.
.	.	.	.	.	.

$(M+1) \times M$ (right) ; $(M+1) \times M$ (bottom)

where $\sum \mathcal{M}^p_{\mathcal{D}_c}$ represents the sum of all entries in the matrix.

According to the directions of the shortest paths, the entries $((s_i,d_i),(s_j,d_j))$ can be separated into four cases: (clockwise, clockwise), (clockwise, anti-clockwise), (anti-clockwise, clockwise) and (anti-clockwise, anti-clockwise). One entry being 1 must be in either (clockwise, clockwise) or (anti-clockwise, anti-clockwise) case.

Now, we calculate the number of entries in (clockwise, clockwise) being 1 as follows. The total of entries of (clockwise, clockwise) is $\binom{M+1}{2}^2$. For each (s_i,d_i), the amount of (s_j,d_j) which do not intersect with it is $\binom{s_i}{2} + \binom{M+2-d_i}{2}$. Therefore, $\#\{entry = 0 | \text{in clockwise}\} = \sum_{s_i=1}^{M}\sum_{d_i=s_i+1}^{M+1}\{\binom{s_i}{2} + \binom{M+2-d_i}{2}\} = \frac{M^4+6M^3+17M^2+12M}{12}$. Thus, $\#\{entry = 1 | \text{in clockwise}\} = \binom{M+1}{2}^2 - \frac{M^4+6M^3+17M^2+12M}{12} = \frac{M^4-7M^2-6M}{6}$. By symmetry, the number of entries in (anti-clockwise, anti-clockwise) being 1 is the same as $\frac{M^4-7M^2-6M}{6}$.

Hence, $p = \frac{M^4-7M^2-6M}{3M^2(M+1)^2} = \frac{M^4-7M^2-6M}{3M^4+6M^3+3M^2} = \frac{1}{3} + o(1)$ ■

2) In the uniform distribution $\mathcal{D}_u$:

Theorem 3: Suppose that an EON $G(V,E)$ is an odd-cycle bidirectional ring with $|V| = 2M+1$ and all of the requests in $\mathcal{R}$ generated from the $\mathcal{D}_u$ and that $\hat{G}(\hat{V},\hat{E})$ is the conflict graph of RF algorithm, then the $\mathbf{E}(|\hat{E}|)$ is $\binom{n}{2}\frac{2M^4+M^3}{8M^4+8M^3+2M^2} = \binom{n}{2}(\frac{1}{4}+o(1))$, where n is the number of requests ($o(1)$ is an infinitesimal of M).

Proof. Similar to the above analysis, we just need to calculate p, the probability that $P_i \cap P_j \neq \emptyset$, where P_i and P_j are the shortest paths for R_i and R_j respectively. Under the uniform distribution, the request pair (R_i,R_j) has a total of $(2M)^2(2M+1)^2$ cases.

We construct a (0-1)-matrix $\mathcal{M}^p_{\mathcal{D}_u}$ as shown in Table III. The top row in Table III represents that all source-destination pairs are routed by shortest paths, and the leftmost column is of the same meaning. One entry $((s_i,d_i),(s_j,d_j))$ of this matrix equals 1 iff the shortest path of (s_i,d_i) intersects with that of (s_j,d_j).

TABLE III
(0-1)-MATRIX $\mathcal{M}^p_{\mathcal{D}_u}$

R_i \ R_j	.	.	(s_j,d_j)	.	.
.	.	.	.	.	.
.	.	.	.	.	.
(s_i,d_i)	.	.	1	.	.
.	.	.	.	.	.
.	.	.	.	.	.

$(2M+1) \times 2M$ (right) ; $(2M+1) \times 2M$ (bottom)

Similarly, we calculate the number of entries in (clockwise, clockwise) being 1 as follows. We separate all of the $\binom{2M+1}{2}$

source-destination pairs (all possible clockwise requests) into M groups according to the length of their shortest paths (edge number) from 1 to M (thus, each group consists of $2M+1$ source-destination pairs). For a source-destination pair with a shortest path of length k, the number of source-destination pairs with a shortest path of length h intersecting with it is $k+h-1$. Therefore, $\#\{entry = 1|\text{in clockwise}\} = \sum_{k=1}^{M} \cdot\{(2M+1) \cdot \sum_{h=1}^{M}(k+h-1)\} = 2M^4 + M^3$. The number of entries in (anti-clockwise, anti-clockwise) being 1 is also $2M^4 + M^3$.

Hence, $p = \dfrac{\sum \mathcal{M}^p_{\mathcal{D}_u}}{(2M)^2(2M+1)^2} = \dfrac{2 \cdot (2M^4+M^3)}{(2M+1)^2 \cdot (2M)^2} = \dfrac{2M^4+M^3}{8M^4+8M^3+2M^2} = \dfrac{1}{4} + o(1)$. ■

B. Conflict Graph of the SF algorithm

For the SF algorithm, the intersection probability of the lightpaths P_i and P_j of any two requests R_i and R_j becomes tricky, because the selection of the lightpaths P_i (R_i) and P_j (R_j) may be affected by the previously selected lightpaths. In other words, the intersecting probability of P_i and P_j depends on not only the EON $G(V,E)$ and the request distribution but also the current status of the EON.

However, given the underlying EON $G(V,E)$ and traffic distribution, the edge number of the conflict graph of the SF algorithm should also follow a certain probability distribution. This point can be exemplified by the example below.

***Example** 1:* We suppose that the EON $G(V,E)$ is a ring (cycle) of three nodes. There are three requests $\mathcal{R} = \{R_1, R_2, R_3\}$, which follow the uniform distribution $\mathcal{D}_u$. For each connection request $R_i(s_i, d_i), 1 \le i \le 3$, there are 6 different choices of source-destination pair, each of which occurs with a probability $\dfrac{1}{6}$. Hence, there are 6^3 combinations in total for (R_1, R_2, R_3), each of which occurs with probability $\dfrac{1}{6^3}$. Each combination of (R_1, R_2, R_3) corresponds to a fixed conflict graph under the process of the SF algorithm. Thus, given an EON and a traffic distribution, the number of the edges of conflict graph of the SF algorithm should also follow a certain distribution, which can be approached by the law of large numbers (LLN) [31].

VII. Numerical Results

In this section, we conduct simulations in elastic optical rings under the following two scenarios and compare the performances of the RF and SF algorithms in terms of the edge numbers of the conflict graphs.

A. Traffic Assumption

1) Traffic Distribution: We utilize the two traffic distributions introduced above to generate the request set in the two scenarios below.

- Concentration distribution $\mathcal{D}_c$ on elastic optical rings
- Uniform distribution $\mathcal{D}_u$ on elastic optical rings

2) Bandwidth Setting: In the classical RSA problem and its resolution algorithms [14, 15], the modulation format is not taken into account, and all requests are assumed to use the same modulation format. Similar to the bandwidth settings in [14, 15], the bandwidth of each request is set in the range of $[\alpha, \beta]$, where α and β are two integers. We simulate each scenario with $\alpha = 1$, $\beta = 2, 3, 4$ respectively, and $GB = 1$. Besides, we have also taken into account the plain RWA case in our simulations. In fact, RWA is actually a special case of the RSA by setting $\alpha = \beta = 4$ and $GB = 0$, since one wavelength (50 GHz) in WDM networks generally takes a size of four FSs (12.5 GHz each). Due to the high complexity, the theoretical analysis of the Routing, Modulation and Spectrum Assignment (RMSA) problem [32] and its associated bandwidth setting with the consideration of modulation formats (*i.e.*,) can be investigated in future work.

The number of requests is set as $n = 1000$ in each simulation. We repeat each simulation 50 times under the same circumstance to ensure sufficient statistical accuracy, and a 95% confidence interval is given to each numerical result. All the simulations have been run by MATLAB 2015a on a computer with 3.2 GHz Intel(R) Core(TM) i5-4690S CPU and 8 GBytes RAM.

B. Simulation Scenarios

1) Concentration Distribution on elastic optical rings: In this scenario, we conduct simulations on 19-cycle, 59-cycle and 99-cycle elastic optical rings respectively, where the number denotes the number of nodes in the ring. These big rings have been used just for sake of theoretical analysis under extreme cases, where the edge number of the RF's conflict graph will converge to the theoretical value calculated in Section VI-A. According to the bandwidth range and the vertex number of the rings (cycles), there are 12 simulation cases as shown in Table IV, which are denoted by labels from A_1 to L_1 respectively.

TABLE IV
Comparison under concentration distribution on elastic optical rings

$n = 1000$	19-cycle	59-cycle	99-cycle
$\beta = 2$	A_1	E_1	I_1
$\beta = 3$	B_1	F_1	J_1
$\beta = 4$	C_1	G_1	K_1
RWA	D_1	H_1	L_1

2) Uniform Distribution on elastic optical rings: In this uniform scenario, we also conduct simulations on 19-cycle, 59-cycle and 99-cycle optical rings respectively. Similar to the previous one, there are also 12 cases as shown in Table V, which are labeled from A_2 to L_2 respectively.

In the two scenarios, since the number of request n is fixed as 1000, instead of directly counting the edge number $\#\{e\}$ of conflict graphs of the two benchmark algorithms, we use $\dfrac{\#\{e\}}{\binom{n}{2}}$ for convenience. Thus, for the RF algorithm, according to Theorems 2 and 3, the $\dfrac{\#\{e\}}{\binom{n}{2}}$ with the growth of

TABLE V
COMPARISON UNDER UNIFORM DISTRIBUTION ON ELASTIC OPTICAL RINGS

$n = 1000$	19-cycle	59-cycle	99-cycle
$\beta = 2$	A_2	E_2	I_2
$\beta = 3$	B_2	F_2	J_2
$\beta = 4$	C_2	G_2	K_2
RWA	D_2	H_2	L_2

vertex number on the ring should converge to $\frac{1}{3}$ and $\frac{1}{4}$ in the concentration and uniform request distributions respectively.

C. Simulation Results

1) Concentration Distribution on elastic optical rings:

The numerical results of final MUFIs, $\frac{\#\{e\}}{\binom{n}{2}}$ and runtime from A_1 to L_1 of the two benchmark algorithms are demonstrated in Figs. 7, 8 and 9 respectively.

Regarding the MUFIs, in $\beta = 2$, $\beta = 3$, $\beta = 4$ and RWA, the means are 699.70, 831.82, 947.74 and 1292.84 respectively for the RF algorithm, while they are 432.46, 523.68, 602.98 and 846.23 respectively for the SF. In other words, the MUFIs of the RF are 61.80%, 58.84%, 57.17% and 52.78% respectively bigger than the SF's in the four cases.

With respect to $\frac{\#\{e\}}{\binom{n}{2}}$ for the RF algorithm, the realistic values converge to the theoretical value calculated in Theorem 2 as vertex number grows in elastic optical rings, *i.e.*, $\frac{1}{3}$, which validates our computing method. For the RF, the mean values of $\frac{\#\{e\}}{\binom{n}{2}}$ in 19-, 59- and 99-cycle are 31.14%, 32.10% and 33.25% respectively while they are 26.34%, 27.41% and 28.06% respectively for the SF. From the analysis above, the more edges the conflict graph contains, the more incompatible these requests, and thus the bigger the final MUFI. The results in Figs. 7 and 8 confirm our assertion that the number of the edges of conflict graph of an RSA algorithm is a pivotal determinant of its final performance. Besides, there is an interesting phenomenon in Fig. 7 that the MUFI seems independent from the node number in the optical rings. This can be explained by the theoretical deductions in Theorems 2 and 3 that the node number of optical rings has an infinitesimal impact on the edge number of the conflict graphs.

Finally, from the aspect of time complexity, the runtime of the SF steeply soars as the number of nodes increases while the runtime of the RF always keeps stable and low as shown in Fig. 9. This shows the drawback of scalability for the SF algorithm.

2) Uniform Distribution on elastic optical rings:

The numerical results of final MUFIs, $\frac{\#\{e\}}{\binom{n}{2}}$ and runtime from A_2 to L_2 by the two benchmark algorithms are demonstrated in Figs. 10, 11 and 12 respectively.

As for the MUFIs, in $\beta = 2$, $\beta = 3$, $\beta = 4$ and RWA, for the RF algorithm, the means are 397.36, 476.83, 558.07 and 771.17 respectively while for the SF 422.46, 516.70, 605.98 and 836.24 respectively. That is the SF's MUFIs are 6.32%,

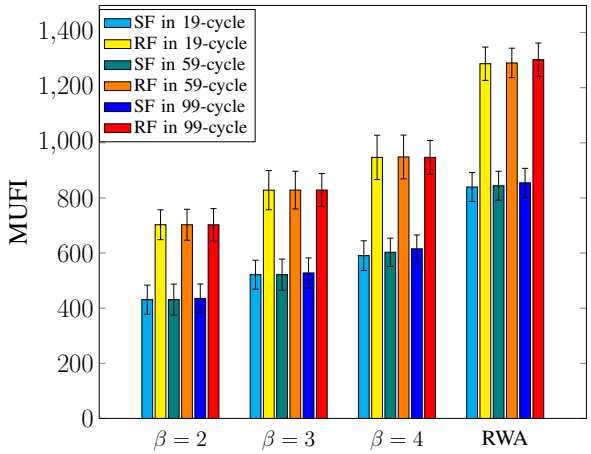

Fig. 7. Numerical results of the concentration distribution on elastic optical rings.

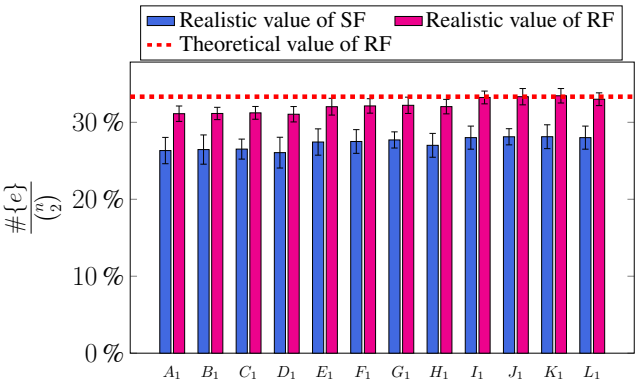

Fig. 8. $\frac{\#\{e\}}{\binom{n}{2}}$ in the 12 cases in TABEL IV.

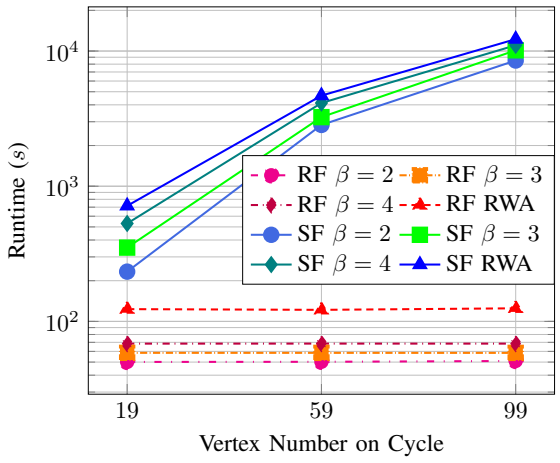

Fig. 9. The runtime of the RF and SF algorithms under the concentration distribution.

8.36%, 8.58% and 8.44% bigger than the RF's MUFIs in respective cases. This results break the notion in the literature that the SF algorithm is always better than the RF and show that the superiority of the two benchmark algorithms varies under different environments.

From aspect of $\frac{\#\{e\}}{\binom{n}{2}}$, for the RF algorithm, with the growth of vertex number of elastic optical rings, the realistic values converge to the theoretical value calculated in Theorem 3, *i.e.*, $\frac{1}{4}$ which further validate our computing method. For the RF, the mean value of $\frac{\#\{e\}}{\binom{n}{2}}$ in 19-, 59- and 99-cycle are 24.05%, 24.70% and 25.00% respectively while for the SF 27.78%, 27.84% and 28.14% respectively. The relations between the edge numbers of the conflict graphs and the final MUFIs in Figs. 10 and 11 further prove the importance of reducing the edge count of conflict graph.

Finally, from the aspect of time complexity, with the growth of vertices on the elastic optical rings, similar to the above, the runtime of the SF is quickly climbing while the RF's runtime always keeps stable and low. Combing with the results in Fig. 10, it manifests that under the uniform distribution, using the SF algorithm is not a wise choice since it needs more time for computation while outputting worse final MUFIs.

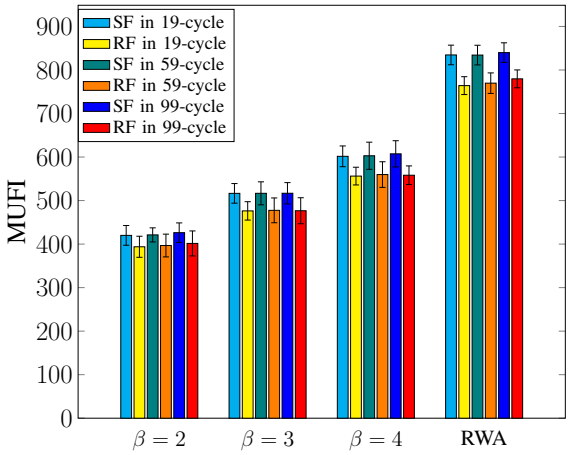

Fig. 10. Numerical results of the uniform distribution on elastic optical rings.

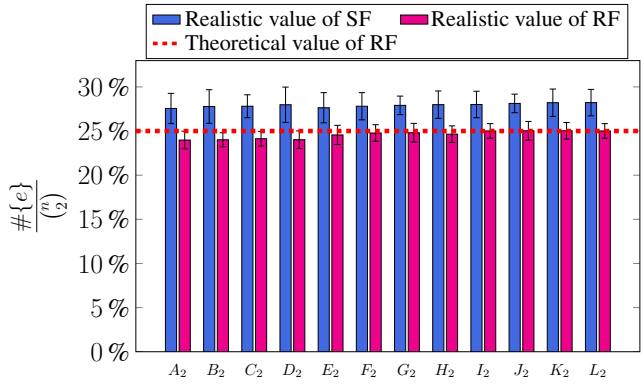

Fig. 11. $\frac{\#\{e\}}{\binom{n}{2}}$ in the 12 cases in TABEL V.

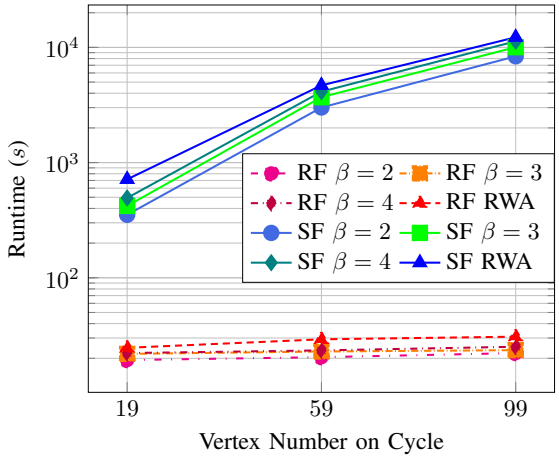

Fig. 12. The runtime of RF and SF algorithms under the uniform distribution.

To sum up, the conflict graph of an RSA algorithm, which varies in different simulation environments, has a decisive impact on the final MUFIs.

VIII. Conclusions

In this work, we focus on the performance evaluation of RSA algorithms rather than proposing a new one. To this end, we developed a unified theoretical analysis framework based on conflict graph. We showed that all RSA algorithms can be viewed as first computing routing paths and then constructing a conflict graph for allocating spectrum resources. Especially, the performance of an RSA algorithm is restricted by the edge number of its conflict graph. To validate the proposed framework, we derived the edge numbers of the conflict graphs built by the RF and the SF algorithms in elastic optical rings. Our theoretical analysis together with the numerical simulations in elastic optical rings show an interesting fact that the RF saves more spectrum resource than the SF in the uniform traffic distribution while the result is inverse in the concentration traffic distribution.

According to the analysis in this paper, we obtained an important observation that there is no one omnipotent RSA algorithm which outperforms the others in all circumstances. This is different from the claims in the literature. Therefore, the selection of RSA algorithms should take into account the traffic distribution and the EON topology so that the conflict graph of the applied RSA algorithm can be as sparse as possible in order to minimize the MUFI.

References

[1] Z. Zhu, W. Lu, L. Zhang, and N. Ansari, "Dynamic service provisioning in elastic optical networks with hybrid single-/multi-path routing," *J. Lightw. Technol.*, vol. 31, pp. 15–22, Jan. 2013.

[2] O. Gerstel, M. Jinno, A. Lord, and B. Yoo, "Elastic optical networking: a new dawn for the optical layer?" *IEEE Commun. Mag.*, vol. 50, pp. s12–s20, Feb. 2012.

[3] P. Lu, L. Zhang, X. Liu, J. Yao, and Z. Zhu, "Highly efficient data migration and backup for big data applications in elastic optical inter-data-center networks," *IEEE Netw.*, vol. 29, pp. 36–42, Sept./Oct. 2015.

[4] M. Jinno, H. Takara, B. Kozicki, Y. Tsukishima, Y. Sone, and S. Matsuoka, "Spectrum-efficient and scalable elastic optical path network: architecture, benefits, and enabling technologies," *IEEE Commun. Mag.*, vol. 47, pp. 66–73, Nov. 2009.

[5] G. Zhang, M. Leenheer, A. Morea, and B. Mukherjee, "A survey on OFDM-based elastic core optical networking," *IEEE Commun. Surveys Tuts.*, vol. 15, pp. 65–87, First Quarter 2013.

[6] F. Ji, X. Chen, W. Lu, J. Rodrigues, and Z. Zhu, "Dynamic p-cycle protection in spectrum-sliced elastic optical networks," *J. Lightw. Technol.*, vol. 32, pp. 1190–1199, Mar. 2014.

[7] W. Fang, M. Lu, X. Liu, L. Gong, and Z. Zhu, "Joint defragmentation of optical spectrum and IT resources in elastic optical datacenter interconnections," *J. Opt. Commun. Netw.*, vol. 7, pp. 314–324, Apr. 2015.

[8] K. Christodoulopoulos, I. Tomkos, and E. Varvarigos, "Elastic bandwidth allocation in flexible OFDM-based optical networks," *J. Lightw. Technol.*, vol. 29, pp. 1354–1366, May. 2011.

[9] L. Gong, X. Zhou, W. Lu, and Z. Zhu, "A two-population based evolutionary approach for optimizing routing, modulation and spectrum assignments (RMSA) in O-OFDM networks," *IEEE Commun. Lett.*, vol. 16, pp. 1520–1523, Sept. 2012.

[10] H. Wu, F. Zhou, Z. Zhu, and Y. Chen, "On the distance spectrum assignment in elastic optical networks," *IEEE/ACM Trans. Netw.*, vol. 25, no. 4, pp. 2391–2404, Aug. 2017.

[11] W. Lu, X. Zhou, L. Gong, M. Zhang, and Z. Zhu, "Dynamic multi-path service provisioning under differential delay constraint in elastic optical networks," *IEEE Commun. Lett.*, vol. 17, no. 1, pp. 158–161, Jan. 2013.

[12] S. Shirazipourazad, C. Zhou, Z. Derakhshandeh, and A. Sen, "On routing and spectrum allocation in spectrum-sliced optical networks," in *Proc. of INFOCOM 2013*, Apr. 2013, pp. 385–389.

[13] B. Chatterjee, N. Sarma, and E. Oki, "Routing and spectrum allocation in elastic optical networks: A tutorial," *IEEE Commun. Surveys Tuts.*, vol. 17, pp. 1776–1800, Third Quarter 2015.

[14] X. Liu, L. Gong, and Z. Zhu, "Design integrated RSA for multicast in elastic optical networks with a layered approach," in *Proc. of GLOBECOM 2013*, Dec. 2013, pp. 2346–2351.

[15] Y. Wang, X. Cao, Q. Hu, and Y. Pan, "Towards elastic and fine-granular bandwidth allocation in spectrum-sliced optical networks," *J. Opt. Commun. Netw.*, vol. 4, pp. 906–917, Nov. 2012.

[16] Z. Zhu, X. Liu, Y. Wang, W. Lu, L. Gong, S. Yu, and N. Ansari, "Impairment- and splitting-aware cloud-ready multicast provisioning in elastic optical networks," *IEEE/ACM Trans. Netw.*, vol. 25, pp. 1220–1234, Apr. 2017.

[17] L. Gong, X. Zhou, X. Liu, W. Zhao, W. Lu, and Z. Zhu, "Efficient resource allocation for all-optical multicasting over spectrum-sliced elastic optical networks," *IEEE J. Opt. Commun. Netw.*, vol. 5, no. 8, pp. 836–847, Aug. 2013.

[18] L. Yang, L. Gong, F. Zhou, B. Cousin, M. Molnar, and Z. Zhu, "Leveraging light-forest with rateless network coding to design efficient all-optical multicast schemes for elastic optical networks," *J. Lightw. Technol.*, vol. 33, pp. 3945–3955, Sept. 2015.

[19] J. Zhu, B. Zhao, and Z. Zhu, "Attack-aware service provisioning to enhance physical-layer security in multi-domain EONs," *J. Lightw. Technol.*, vol. 34, pp. 2645–2655, Jun. 2016.

[20] Y. Yin, H. Zhang, M. Zhang, M. Xia, Z. Zhu, S. Dahlfort, and S. Yoo, "Spectral and spatial 2D fragmentation-aware routing and spectrum assignment algorithms in elastic optical networks," *J. Opt. Commun. Netw.*, vol. 5, pp. A100–A106, Oct. 2013.

[21] W. Shi, Z. Zhu, M. Zhang, and N. Ansari, "On the effect of bandwidth fragmentation on blocking probability in elastic optical networks," *IEEE Trans. Commun.*, vol. 61, pp. 2970–2978, Jul. 2013.

[22] M. Zhang, C. You, and Z. Zhu, "On the parallelization of spectrum defragmentation reconfigurations in elastic optical networks," *IEEE/ACM Trans. Netw.*, vol. 24, pp. 2819–2833, Oct. 2016.

[23] S. Ba, B. Chatterjee, and E. Oki, "Defragmentation scheme based on exchanging primary and backup paths in 1+1 path protected elastic optical networks," *IEEE/ACM Trans. Netw.*, vol. 25, no. 3, pp. 1717–1731, Jun. 2017.

[24] B. Chatterjee, S. Ba, and E. Oki, "Fragmentation problems and management approaches in elastic optical networks: A survey," *IEEE Commun. Surveys Tuts.*, vol. 20, no. 1, pp. 183–210, Firstquarter 2018.

[25] L. Gong and Z. Zhu, "Virtual optical network embedding (VONE) over elastic optical networks," *J. Lightw. Technol.*, vol. 32, pp. 450–460, Feb. 2014.

[26] B. Jaumard and M. Daryalal, "Efficient spectrum utilization in large scale RWA problems," *IEEE/ACM Trans. Netw.*, vol. 25, no. 2, pp. 1263–1278, Apr. 2017.

[27] B. Mukherjee, *Optical WDM Networks (Optical Networks)*. Berlin, Heidelberg: Springer-Verlag, 2006.

[28] H. Zang, J. Jue, and B. Mukherjee, "A review of routing and wavelength assignment approaches for wavelength-routed optical WDM networks," *Opt. Netw. Mag.*, pp. 47–60, 2000.

[29] X. Dong, T. El-Gorashi, and J. Elmirghani, "On the energy efficiency of physical topology design for ip over wdm networks," *J. Lightw. Technol.*, vol. 30, no. 12, pp. 1931–1942, Jun. 2012.

[30] M. Ju, F. Zhou, S. Xiao, and Z. Zhu, "Power-efficient protection with directed p -cycles for asymmetric traffic in elastic optical networks," *J. Lightw. Technol.*, vol. 34, no. 17, pp. 4053–4065, Sept. 2016.

[31] G. Grimmett and D. Stirzaker, *Probability and Random Processes, 2nd Edition*. Clarendon Press, Oxford, 1992.

[32] F. S. Abkenar and A. G. Rahbar, "Study and Analysis of Routing and Spectrum Allocation (RSA) and Routing, Modulation and Spectrum Allocation (RMSA) Algorithms in Elastic Optical Networks (EONs)," *Opt. Switch. Netw.*, vol. 23, pp. 5 – 39, 2017.